

## DELAYED BIFURCATION AT THE THRESHOLD OF A SWEEPED GAIN CO<sub>2</sub> LASER

F.T. ARECCHI<sup>1</sup>, W. GADOMSKI<sup>2</sup>, R. MEUCCI and J.A. ROVERSI<sup>3</sup>

*Instituto Nazionale di Ottica, 50125 Firenze, Italy*

Received 28 June 1988

A single mode CO<sub>2</sub> laser near threshold behaves differently depending on whether the threshold is reached by varying the pump or the cavity losses. Only in the first case we observe a delayed bifurcation. Our experimental results are explained by a four level molecular model which takes into account the coupling between the two resonant levels and the rotational manifold.

### 1. Introduction

Theoretical studies of the semiclassical laser equations for two-level atoms predict the appearance of a delayed bifurcation when the pump parameter is swept linearly in time across the threshold region [1]. Recently, such a delayed bifurcation has been observed by Scharpf et al. [2] at the threshold of an Ar<sup>+</sup> laser by varying the cavity losses. In contrast, in a previous paper we reported that there was no delay of the bifurcation at threshold in a CO<sub>2</sub> laser when the cavity loss was varied linearly in time [3].

In this paper we report on a delayed bifurcation of a CO<sub>2</sub> laser when the pump parameter is swept across the threshold region, and explain the difference with the above mentioned case.

The experimental data show that the delay of the bifurcation is independent of how far below threshold the laser is brought by a triangular modulation, apart from a sharp transition to zero very near to threshold. We show that numerical results for triangular pump modulation for both two- and four-level models predict the same behavior at the bifurcation. However, our data are better described in terms of the four-level model, because it provides a fast damping of the oscillations as experimentally observed. Moreover, this latter model is consistent

with the data obtained by loss modulation [3] where the two-level model would instead predict an unobserved delay.

### 2. Experimental results

The experimental set-up is shown in fig. 1. It consists of a CO<sub>2</sub> laser tube, with Brewster angle windows, placed inside a confocal resonator 2.5 m long. One of the reflectors of the laser cavity is a grating mounted in autocollimation configuration, in order to select the P(20) line at 10.6 μm; the other is a partially reflecting Ge mirror (R=80%) with a 5 m radius of curvature. The coupling mirror is mounted

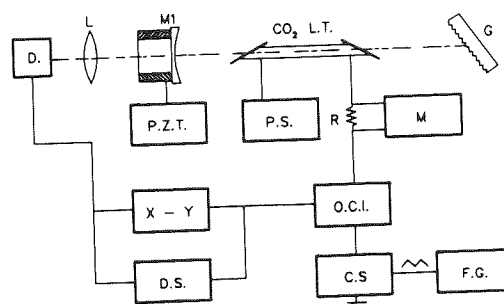


Fig. 1. Experimental set-up with a CO<sub>2</sub> laser. M1, partially reflecting Ge mirror mounted on a piezo translator; G, grating (100 lines / mm); D, HgCdTe detector; R, precision resistor; M, D.C. meter; P.S., high voltage power supply; O.C.I., optically coupled isolator whose output is proportional to the discharge current; C.S., current stabilizer; F.G., function generator (triangular wave).

<sup>1</sup> Also Dept. of Physics, University of Florence, Italy

<sup>2</sup> Permanent address: Warsaw University, Warsaw, Poland

<sup>3</sup> Permanent address: Universidade Estadual de Campinas, Campinas, S.P., Brasil

on a hollow cylindrical piezo-electric-translator (PZT) in order to control the detuning between the center of molecular line and the frequency of the cavity mode.

The in-flow CO<sub>2</sub> laser is pumped by means of a DC discharge. The power supply is current stabilized to better than 0.05%. The discharge length is 0.8 m and the gas mixture is composed of CO<sub>2</sub> (15.4%), H<sub>2</sub> (2.0%), N<sub>2</sub> (14.2%) and He (68.4%) at a total pressure of 25 mbar, measured at the gas inlet of the laser tube. The electronic circuit for the current regulation can be externally modulated around a pre-selected value of the discharge current which is measured on a precision resistor R. The current modulation is monitored directly with an optically coupled isolator in series with the regulator. The laser output intensity is detected by a liquid N<sub>2</sub> cooled HgCdTe detector with a rise time  $\tau \leq 10$  ns. The photodetector signal is sent together with the current modulation signal to an X-Y oscilloscope display and to a digital oscilloscope to monitor the temporal evolution.

In fig. 2a we report the time evolution of the laser intensity and the corresponding current modulation around a mean value of the discharge current ( $5.156 \pm 0.002$ ) mA and at a modulation frequency of 100 Hz. In fig. 2b we report an expanded version of the associated X-Y plot, near the threshold region. As can be seen, in the operating range of current, the laser intensity is not linear as a function of the excitation current, but near threshold the dependence is approximately linear indicating that a linear current sweep near threshold corresponds to a linear sweep of the pump parameter. The stationary threshold current is ( $3.94 \pm 0.02$ ) mA. Calling  $A(t)$  the current normalized to the stationary threshold value, we denote by  $A(0)$  ( $\leq 1$ ) the minimum  $A$  value, by  $A(\bar{t}) = 1$  the threshold value, by  $A(t^*)$  the pump value at which the laser switches-on and by  $A_{\max}$  the maximum value of  $A(t)$ . The sweep rate of the pump parameter is given by  $2 [A_{\max} - A(0)]f$ , where  $f$  is the sweep frequency.

The width of the bistable region defined as  $\Delta A = A(t^*) - A(\bar{t})$ , is unequivocally defined because the switch-on of the laser is characterized by a sharp peak with few damped relaxation oscillations. The dependences of  $\Delta A$  and  $t_d = t^* - \bar{t}$  on the modulation

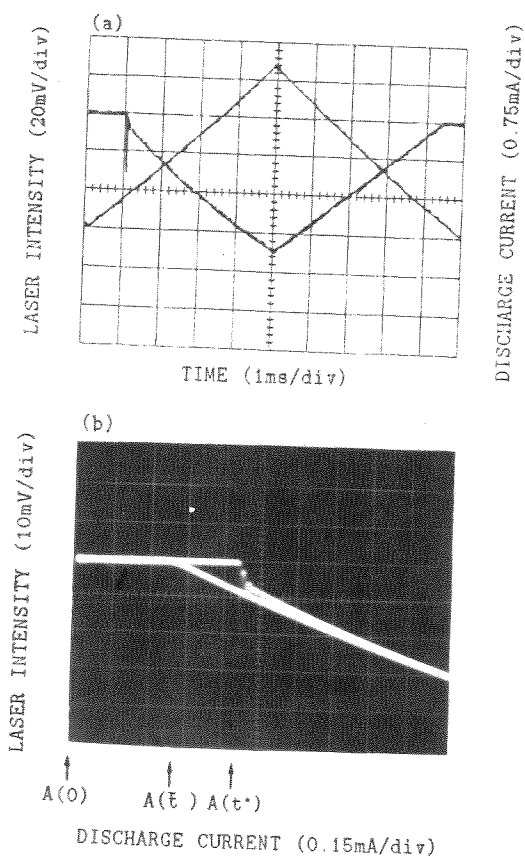


Fig. 2. (a) Laser intensity and discharge current versus time. (b) Amplified version of the corresponding X-Y plot near threshold. The width of the bistable region  $\Delta A = A(t^*) - A(\bar{t})$  is 0.07,  $A(0) = 0.90$  and  $A_{\max} = 1.7$ .

frequency (for fixed modulation amplitude) are shown in figs. 3a and 3b.

The main feature of this delayed bifurcation, at a given sweep frequency and modulation amplitude, is the independence of  $\Delta A$  on  $A(0)$ , when  $A(0) \leq 0.96$ , as shown in fig. 3c.

### 3. Theoretical analysis

The reported results can be explained in terms of a four-level molecular model [4,5] in which the two energy levels are coupled to all other rotational levels of the same vibrational  $\nu$  band. This model was shown previously [3] to be necessary in order to ex-

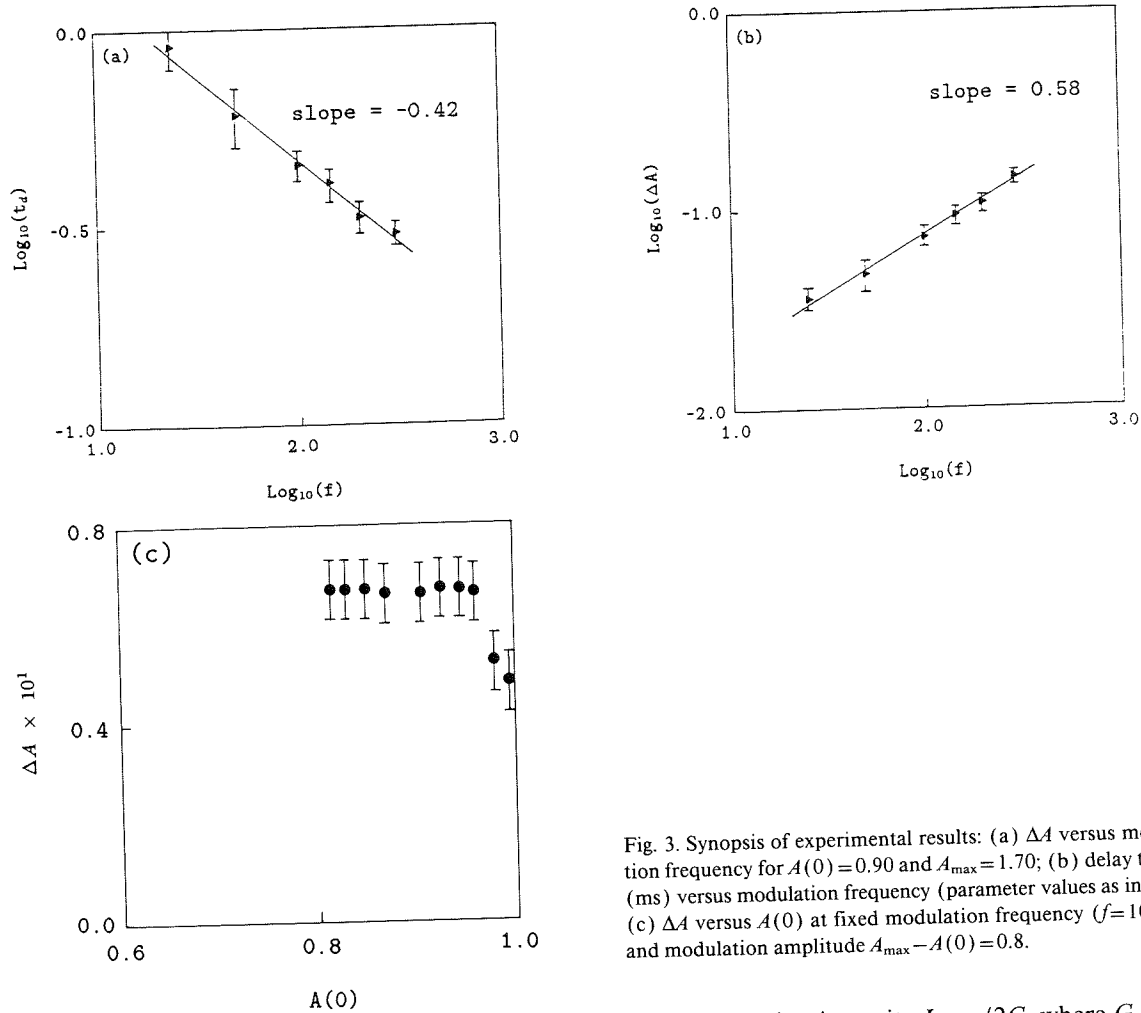


Fig. 3. Synopsis of experimental results: (a)  $\Delta A$  versus modulation frequency for  $A(0)=0.90$  and  $A_{max}=1.70$ ; (b) delay time  $t_d$  (ms) versus modulation frequency (parameter values as in (a)); (c)  $\Delta A$  versus  $A(0)$  at fixed modulation frequency ( $f=100\text{Hz}$ ) and modulation amplitude  $A_{max}-A(0)=0.8$ .

plain the results of loss modulation. It consists of three equations describing the intensity ( $x$ ), the population inversion of the resonant levels ( $y$ ) and the population inversion of the vibrational band ( $z$ ) as follows,

$$\dot{x} = -k_0 x (1 - y), \tag{1}$$

$$\dot{y} = -(\gamma_R + \gamma_{||}) y + \gamma'_R z - \mu x y + \eta \gamma_{||} y_0(t), \tag{2}$$

$$\dot{z} = -(\gamma'_R + \gamma_{||}) z + \gamma_R y + (Z - 1) \eta \gamma_{||} y_0(t), \tag{3}$$

where  $\mu = \gamma_{||}(\gamma_R + \gamma'_R + \gamma_{||}) / (\gamma'_R + \gamma_{||})$  and  $\eta = (\gamma_R + \gamma'_R + \gamma_{||}) / (\gamma_R + \gamma_{||})$ ,  $\gamma_{||}$  is the decay rate from the band  $(\nu, J)$  to  $(\nu', J')$  for  $\nu' \neq \nu$ ,  $\gamma_R$  and  $\gamma'_R$  are the decay rates from resonant level  $(\nu, J)$  to the vibrational band  $(\nu, J')$  (for all  $J' \neq J$ ) and for the reverse process, respectively. The intensity  $x(t)$  is normalized

to the saturation intensity  $I_s = \mu / 2G$ , where  $G$  is the field-matter coupling constant. Both  $y(t)$  and  $z(t)$  are normalized to the threshold inversion  $k_0 / G$ , where  $k_0 = (c / 2L) |\ln R|$  for mirror reflectivity  $R$  and cavity length  $L$ . The last term in each of eqs. (2) and (3) is obtained from ref. [3] via the equilibrium conditions and assuming that the the pump energy is equally distributed among all levels of the vibrational band.

In the numerical calculations we have used  $k_0 = 1.2 \times 10^7 \text{ s}^{-1}$ ,  $R = 0.75$ ,  $\gamma_R = 1.0 \times 10^7 \text{ s}^{-1}$ ,  $\gamma'_R = \gamma_R / Z$ , with  $Z = 16$ , where  $Z + 1$  is an effective multiplicity factor of the vibrational upper band, and the time dependent pump parameter  $y_0(t)$  is a linear function of time of the type  $A(t) = A(0) + \alpha t (\text{sign} [\sin 2\pi f t])$ , with

$$\alpha = [A_{\max} - A(0)] / (T/2)$$

$$= 2[A_{\max} - A(0)] f.$$

In fig. 4 we report numerical solutions of the laser intensity versus the pump parameter for increasing values of the sweep frequency (from 20 Hz to 100 Hz) with constant modulation amplitude. Numerical calculations for pump modulation on the two-level model give similar delay, however, with long damped oscillations (fig. 4d) never observed in the experiment (see fig. 2). A way to increase the damping rate in the two-level model is to increase the decay rate of the population inversion to a value of two orders of magnitude larger than that reported in the literature. Notice that, for such an artificial rate, the two-

level model predicts a delay also for loss modulation, at variance with the experiment (fig. 2 of ref. [3]).

The main features of the bifurcation delays are summarized in figs. 5. In fig. 5a we report  $\log(\Delta A)$  versus  $\log(f)$ , where  $f$  is the frequency in Hz, for two values of  $\gamma_{\parallel}$  ( $0.5 \times 10^4 \text{ s}^{-1}$  and  $1.0 \times 10^4 \text{ s}^{-1}$ ). The slopes of curves (1) and (2) are 0.70 and 0.67, respectively. In fig. 5b we show the behavior of  $\log(t_d)$  versus  $\log(f)$  with slopes for low frequency around  $-0.35$ . The dependence of the decay time  $t_d$  on  $A(0)$  at a given sweep frequency and modulation amplitude is seen in fig. 5c. As can be seen, for  $A(0) \leq 0.97$ ,  $t_d$  is independent of  $A(0)$ , in agreement with the experimental data of fig. 3c.

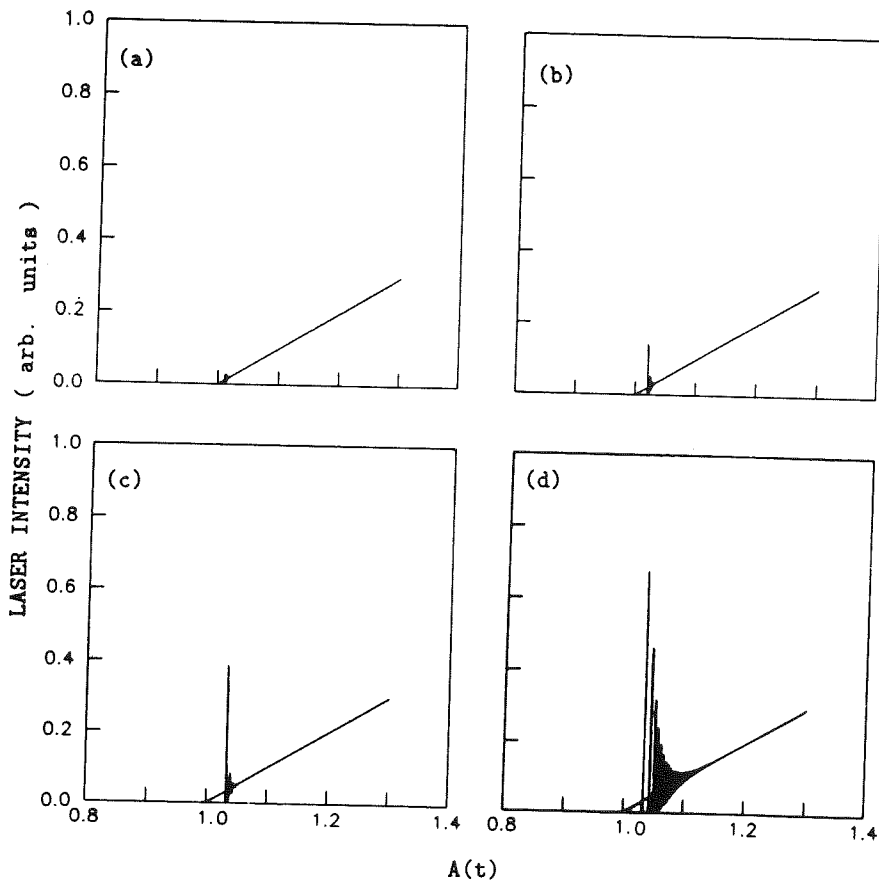


Fig. 4. Numerical results for the four- and two-level model. (a), (b) and (c), (four-level model). Plots of intensity versus  $A(t)$  for modulation frequency  $f=20$  Hz, 50Hz and 100 Hz, respectively.  $\gamma_R=0.5 \times 10^7 \text{ s}^{-1}$  and  $\gamma_{\parallel}=1.0 \times 10^4 \text{ s}^{-1}$ ,  $k_0=1.5 \times 10^7 \text{ s}^{-1}$ ,  $T=0.25$ ,  $A(0)=0.80$ ,  $Z=16$ ,  $A_{\max}-A(0)=0.5$ . (d) The two-level model with the same parameters as above at  $f=100$  Hz.

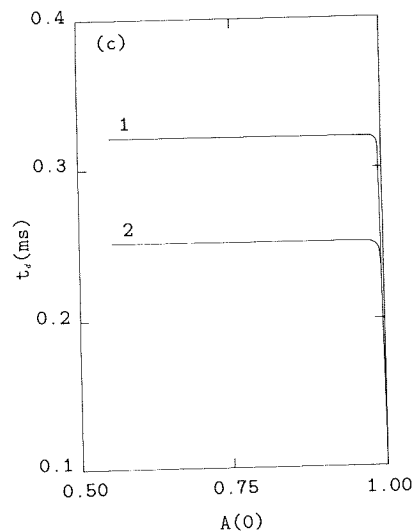
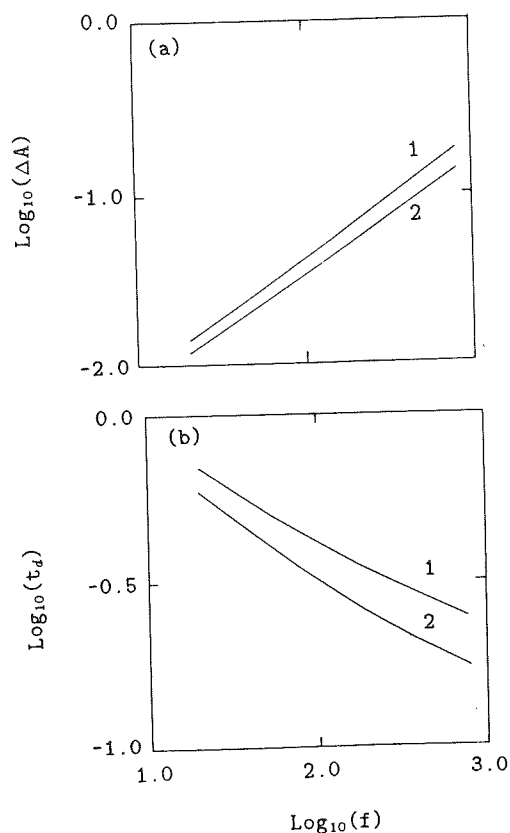


Fig. 5. Synopsis of theoretical results:  $\Delta A$  (a) and  $t_d$  (b) versus  $f$ ; 1 and 2 refer to  $\gamma_{\parallel} = 0.5 \times 10^4$  and  $1.0 \times 10^4 \text{ s}^{-1}$ , respectively. The other parameters are the same as in fig. 4. (c)  $t_d$  versus  $A(0)$  for  $\gamma_R = 10^7 \text{ s}^{-1}$  (other parameters as in (a) and (b)). 1 and 2 correspond to  $f = 100$  and  $200 \text{ Hz}$  respectively.

#### 4. Conclusion

Theoretical results on two-level laser systems predict the same form of delayed bifurcations for either pump or loss swept across the threshold region.

When these two modulation are applied at the threshold region of a  $\text{CO}_2$  laser, a delayed bifurcation arises only for pump modulation. This fact can be explained by considering the essential role played by the relaxation processes ( $\gamma_R, \gamma'_R$ ) between the two resonant levels and the whole rotational manifold. These processes are two orders of magnitude faster than the relaxation rate  $\gamma_{\parallel}$  of the rotational manifold. When the cavity loss parameter is swept across the threshold at a fixed pump value, the fast relaxation processes re-adjust the population inversion between the two resonant levels preventing a delayed response on the time scale of the slow modulation ( $f \leq \gamma_{\parallel}$ ). On the other hand, in the case of pump modulation the excitation process must excite the

whole rotational manifold (at a rate  $\gamma_{\parallel}$ ), so that a delay in the switch-on of the laser of the order of magnitude  $\gamma_{\parallel}^{-1}$ , is observable.

#### Acknowledgement

The authors thank N.B. Abraham for helpful discussions and M. Ciofini and L. Pezzati for help in measurements. One of us (J.A.R.) has a fellowship of CNP<sub>q</sub> (National Research Council of Brazil). This work was partly supported by the European Economic Community. W.G. was supported in part by the Polish Ministry of Science and Higher Education under project CPBP 01.06.

#### References

- [1] P. Mandel and T. Erneux, Phys. Rev. Lett. 53 (1984) 1818;  
P. Mandel, Optics Comm. 64 (1987) 549.

- [2] W. Scharpf, M. Squicciarini, D. Bromley, C. Green, J.R. Tredicce and L.M. Narducci, *Optics Comm.* 63 (1987) 344.
- [3] F.T. Arecchi, W. Gadomski, R. Meucci and J.A. Roversi, *Optics Comm.* 65 (1988) 47.
- [4] J. Dupré, F. Meyer and C. Meyer, *Phys. Rev. Appl. (Paris)* 10 (1975) 285.
- [5] E. Arimondo, F. Casagrande, L.A. Lugiato and P. Glorieux, *Appl. Phys. B* 30 (1983) 57.